ELECTRONIC SUPPORTING INFORMATION (ESI)

for

Serendipitous formation of oxygen-bridged Cu^{II}_6M ($M = Mn^{II}$, Co^{II}) double cubanes showing electrocatalytic water oxidation

Anna Carissa M. San Esteban, Naoto Kuwamura, Nobuto Yoshinari and Takumi Konno*

Department of Chemistry, Graduate School of Science, Osaka University, Toyonaka, Osaka 560-0043, Japan

E-mail: konno@chem.sci.osaka-u.ac.jp

General methods.

$[Cu_2Pt_2(NH_3)_4(D\text{-pen})_4]$ and $[Cu_7(\mu_3\text{-}OH)_6(\mu_3\text{-}Br)_2(D\text{-pends})_3]$ ($\mathbf{1^{Cu}}$) were prepared according to previously reported methods. [S1, S2] IR spectra were measured with a JASCO FT/IR-4100 infrared spectrophotometer using KBr disks. The elemental analyses (C, H, N) were performed at Osaka University using a Yanaco CHN Corder MT-6. High-quality powder X-ray diffraction patterns were recorded at room temperature in transmission mode (synchrotron radiation λ = 1.0 Å; 2θ range = 2-78°; step width = 0.01°; data collection time = 1 min) on a diffractometer equipped with a MYTHEN microstrip X-ray detector (Dectris Ltd) at the SPring-8 BL02B2 beamline. Crystals were loaded into a glass capillary tube (diameter = 0.3 mm) together with a mother liquor, which was rotated during the measurements. Powder simulation patterns were obtained from the single-crystal X-ray structures using Mercury 3.10. Magnetic measurements were carried out using a Quantum-Design MPMS XL7AC SQUID magnetometer. The observed magnetic moment data were corrected for the diamagnetic contribution (χ_{dia}) by the equation $\chi_{dia} = -1/2 \times M \times 10^{-6}$ emu/mol.

X-ray crystal structure determination.

Synchrotron X-ray diffraction studies of $\mathbf{1^{Mn}}$ and $\mathbf{1^{Co}}$ were carried out at the BL02B1 beamline in SPring-8. A PILATUS3 X CdTe 1 M detector was used. The intensity data were collected in ω-scan mode, and empirical absorption corrections were applied. The structures of the complexes were solved by a direct method using SHELXS-2018. [S3] The structure refinements were carried out using full-matrix least squares in SHELXL-2018/1. [S3] All calculations were performed using the Yadokari-XG software package.[S4] All non-hydrogen atoms were refined anisotropically, while H atoms were refined isotropically. H atoms were placed at the calculated positions except for water molecules, which were modelled using DFIX restraints. For $\mathbf{1_{Mn}}$, the initial structural analysis indicated that the asymmetric unit contains one heptanuclear $[Cu_6Mn(OH)_6Br_2(D\text{-pends})_3]$ and 20.5 water molecules of crystallization. Of the 20.5 water molecules, 13.5 water molecules were excluded from the model using the SQUEEZE program to improve the data quality. The SQUEEZE report indicated that the void space is 394 $Å^3$ per asymmetric unit, which matches well with the expected volume of 405 $Å^3$ (30 $Å^3 \times 13.5$) for 13.5 water molecules. For $\mathbf{1_{Co}}$, the initial structural analysis indicated that the asymmetric unit contains two heptanuclear $[Cu_6Co(OH)_6Br_2(D\text{-pends})_3]$ and 41 water molecules of crystallization. Of the 41 water molecules, 29 water molecules were excluded from the model using the SQUEEZE program. The SQUEEZE report indicated that the void space is 848 $Å^3$ per asymmetric unit, which also matches well with the expected volume of 870 $Å^3$ (30 $Å^3 \times 29$) for 29 water molecules. The crystallographic data are summarized in Table S1. The X-ray crystallographic coordinates for the structures reported in this article have been deposited at the Cambridge Crystallographic Data Centre (CCDC) under deposition numbers CCDC 2130570-2130571. These data can be obtained free of charge from the Cambridge Crystallographic Data Centre via www.ccdc.cam.ac.uk/data_request/cif.

Electrocatalytic measurements.

Voltammetry and controlled potential electrolysis were carried out using a CHI600E potentiostat in a three-electrode cell under an Ar atmosphere at room temperature. A sample-modified glassy carbon electrode (ϕ 3.0 mm) was utilized as the working electrode and was prepared by drying 5 μL of sample suspension (2 mg in 200 μL acetonitrile) on the electrode surface and coating with a thin layer of lower aliphatic alcohols/water containing 5% Nafion® (Aldrich). The counter electrode used was a platinum wire, and the reference electrode was a Ag/AgCl (3.0 M NaCl aq.) electrode. The potential where the catalytic current starts to rise was used as the onset potential. Gas chromatography (GC) measurements were performed using a Shimadzu GC-2014 with a thermal conductivity detector operating at 40°C. A 200 μL headspace sample was analysed during electrolysis at +1.3 V. Ar was used as the carrier gas, and O_2 gas was detected on an activated molecular sieve column (ShincarbonST, Restek). The total amount of charge consumption (Q) was obtained from controlled-potential electrolysis after 15 min. The total amount of oxygen gas (a) was obtained from GC measurements after 15 min. Faraday efficiencies (FEs) for O_2 evolution were calculated as a / (Q / nF), where n is the number of transferred electrons and F is the Faraday constant. TOF values were calculated as $a \times 900$ / ($0.00005 \times n$ / Mw), where Mw is the molecular weight of the coordination compound.

Preparation of $[Cu_6Mn(\mu_3\text{-}OH)_6(\mu_3\text{-}Br)_2(D\text{-}pends)_3]$ ($\mathbf{1^{Mn}}$).

To a black solution of $[Cu_2Pt_2(NH_3)_4(D\text{-}pen)_4]$ (0.080 g, 0.058 mmol) in water (6 mL) was added $MnBr_2{\cdot}4H_2O$ (330 mg, 1.15 mmol) dissolved in water (2 mL). The mixture was stirred at room temperature for 10 minutes, followed by allowing it to stand at room temperature. Blue prismatic crystals ($\mathbf{1^{Mn}}$) that appeared were collected by filtration after one week. Yield: 10 mg (26%). Calcd. for $[Cu_6Mn(\mu\text{-}OH)_6(\mu\text{-}Br)_2(D\text{-}pends)_3]{\cdot}20H_2O$: C, 18.56; H, 5.19; N, 4.33%. Anal. Found: C, 18.59; H, 5.00; N, 4.39%. IR (KBr): 1636 (ν_{COO^-}) cm^{-1}. One of the crystals thus obtained was used for single-crystal X-ray crystallography.

Preparation of $[Cu_6Co(\mu_3\text{-}OH)_6(\mu_3\text{-}Br)_2(D\text{-}pends)_3]$ ($\mathbf{1^{Co}}$)

To a black solution of $[Cu_2Pt_2(NH_3)_4(D\text{-}pen)_4]$ (0.080 g, 0.058 mmol) in water (6 mL) was added $CoBr_2{\cdot}6H_2O$ (38 mg, 0.12 mmol) dissolved in water (2 mL). The solution was stirred at room temperature for 10 minutes, followed by allowing it to stand at room temperature. Blue prismatic crystals ($\mathbf{1^{Co}}$) that appeared were collected by filtration after two weeks. Yield: 6 mg (17%). Calcd. for $[Cu_6Co(\mu\text{-}OH)_6(\mu\text{-}Br)_2(D\text{-}pends)_3]{\cdot}16.5H_2O$: C, 19.14; H, 4.98; N, 4.46%. Anal. Found: C, 19.14; H, 5.17; N, 4.44%. IR (KBr): 1636 (ν_{COO^-}) cm^{-1}. One of the crystals thus obtained was used for single-crystal X-ray crystallography.

References.

[S1] N. Kuwamura, Y. Kurioka, N. Yoshinari and T. Konno, *Chem. Commun.*, 2018, **54**, 10766.

[S2] A. Igashira-Kamiyama, J. Fujioka, S. Mitsunaga, M. Nakano, T. Kawamoto and T. Konno, *Chem. Eur. J.*, 2008, **14**, 9512.
[S3] G. M. Sheldrick, *Acta Crystallogr., Sect. C: Struct. Chem.* 2015, **A71**, 3.
[S4] C. Kabuto, S. Akine, T. Nemoto and E. Kwon, *Nippon Kessho Gakkaishi* 2009, **51**, 218.

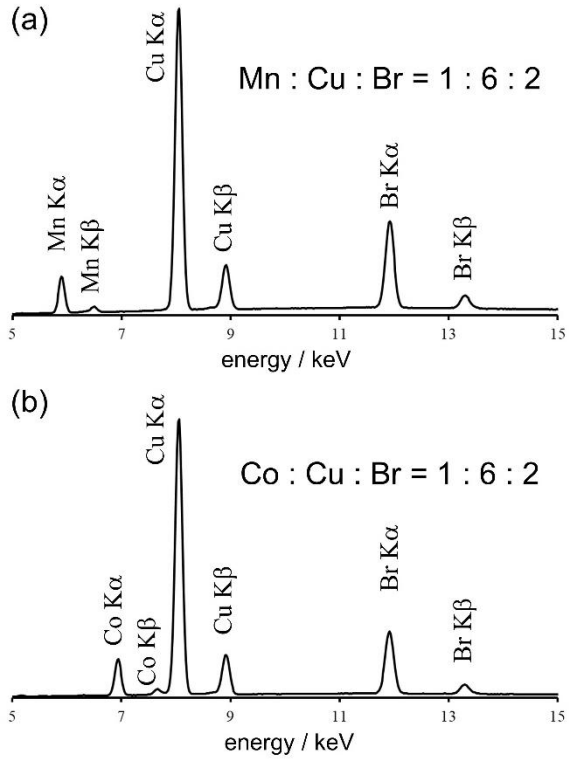

Fig. S1. Fluorescence X-ray spectra of (a) $\mathbf{1^{Mn}}$ and (b) $\mathbf{1^{Co}}$ in the range of 5-15 keV. The signals due to Pt atom (Lα 9.441 eV, Lβ 11.069, 11.249 eV) were not detected.

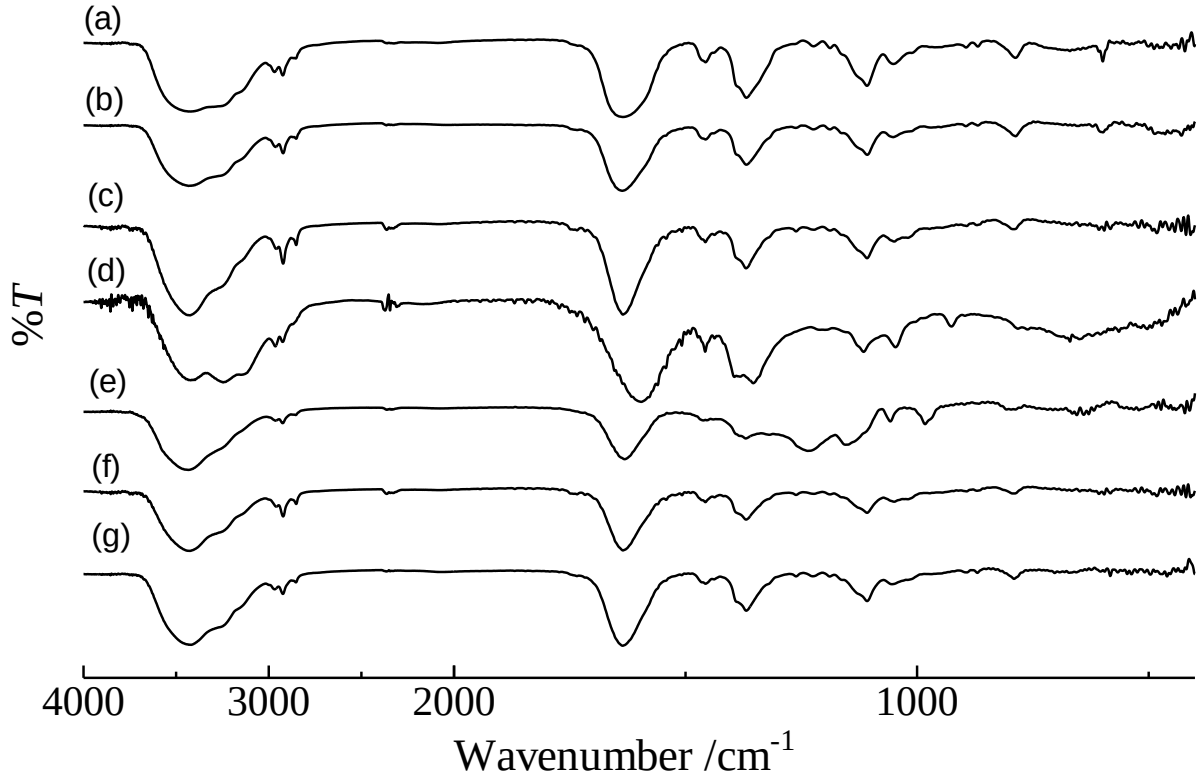

Fig. S2. IR spectra of the original samples of (a) $\mathbf{1^{Mn}}$, (b) $\mathbf{1^{Co}}$, (c) $\mathbf{1^{Cu}}$ and (d) $[Cu_2Pt_2(NH_3)_4(D\text{-pen})_4]$, and IR spectra after bulk electrolysis at +1.3 V of (e) $\mathbf{1^{Mn}}$, (f) $\mathbf{1^{Co}}$ and (g) $\mathbf{1^{Cu}}$.

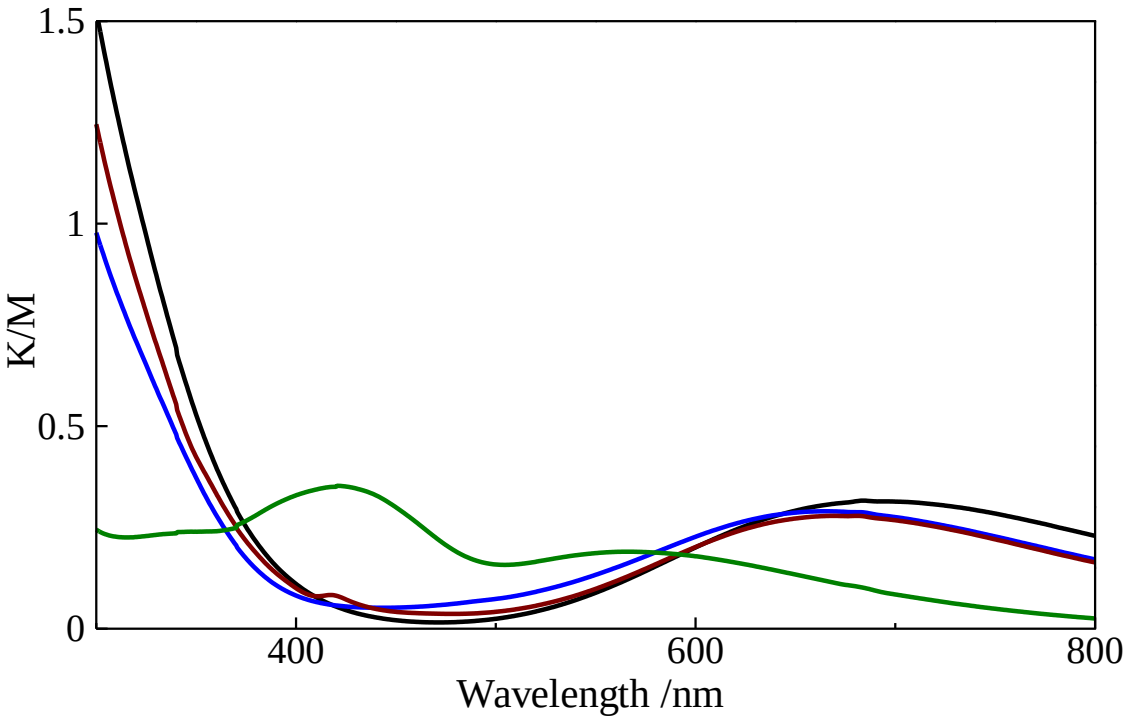

Fig. S3. Diffuse reflectance spectra of (red) $\mathbf{1}^{\mathbf{Mn}}$, (blue) $\mathbf{1}^{\mathbf{Co}}$, (black) $\mathbf{1}^{\mathbf{Cu}}$ and (green) $[Cu_2Pt_2(NH_3)_4(D\text{-}pen)_4]$.

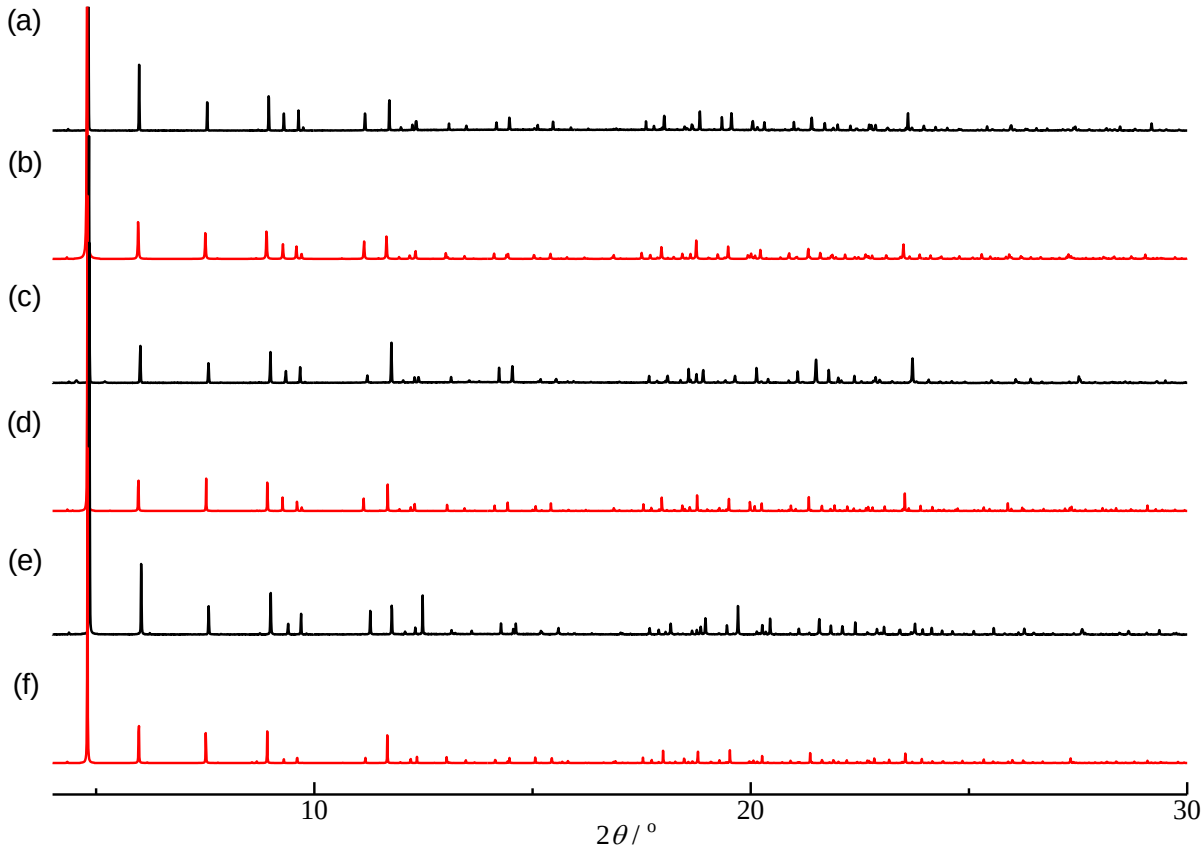

Fig. S4. Experimental (black) and simulated (red) PXRD patterns of (a, b) $\mathbf{1}^{\mathbf{Mn}}$, (c, d) $\mathbf{1}^{\mathbf{Co}}$ and (e, f) $\mathbf{1}^{\mathbf{Cu}}$.

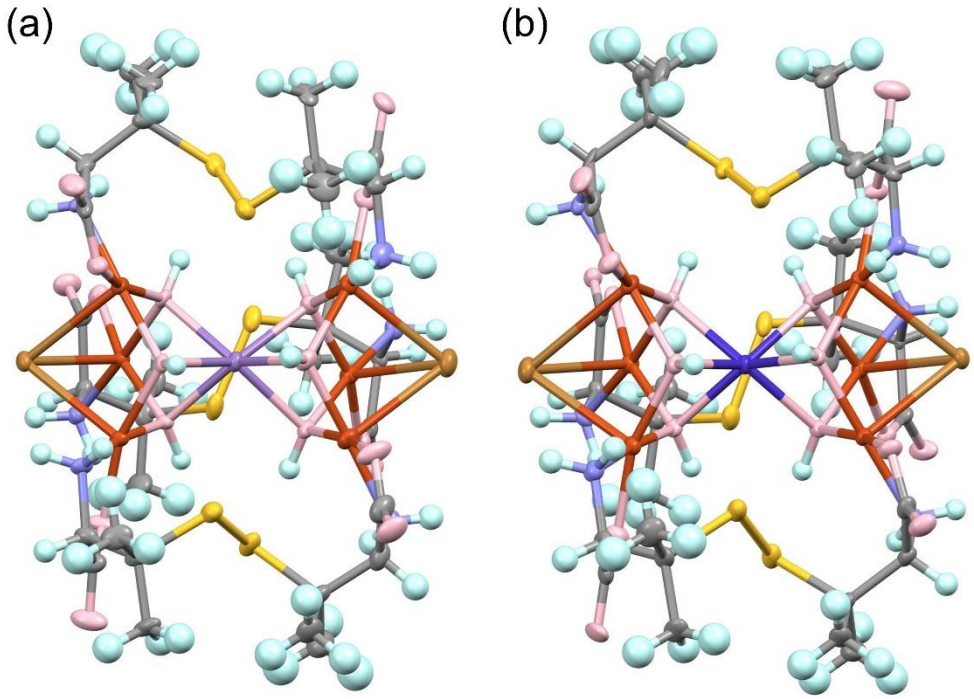

Fig. S5. Perspective views of (a) $\mathbf{1}^{\mathbf{Mn}}$ and (b) $\mathbf{1}^{\mathbf{Co}}$ in the thermal ellipsoid model with the 50% probability. Colour codes: pale purple, Mn; blue, Co; brown Cu; yellow S; ochre Br; pink O; light blue N; grey C; pale blue H. Water molecules are omitted for clarity. One of two crystallographically independent molecules is illustrated for $\mathbf{1}^{\mathbf{Co}}$.

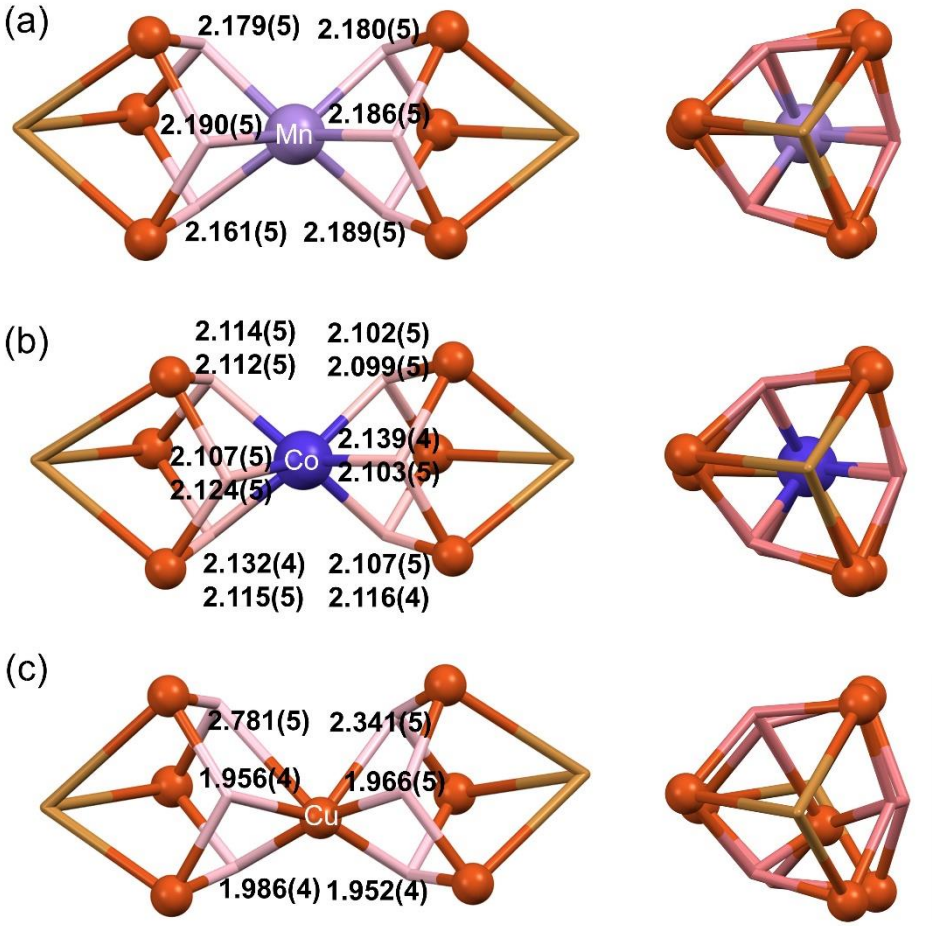

Fig. S6. Double-cubane frameworks in (a) $\mathbf{1}^{\mathbf{Mn}}$, (b) $\mathbf{1}^{\mathbf{Co}}$ and (c) $\mathbf{1}^{\mathbf{Cu}}$.

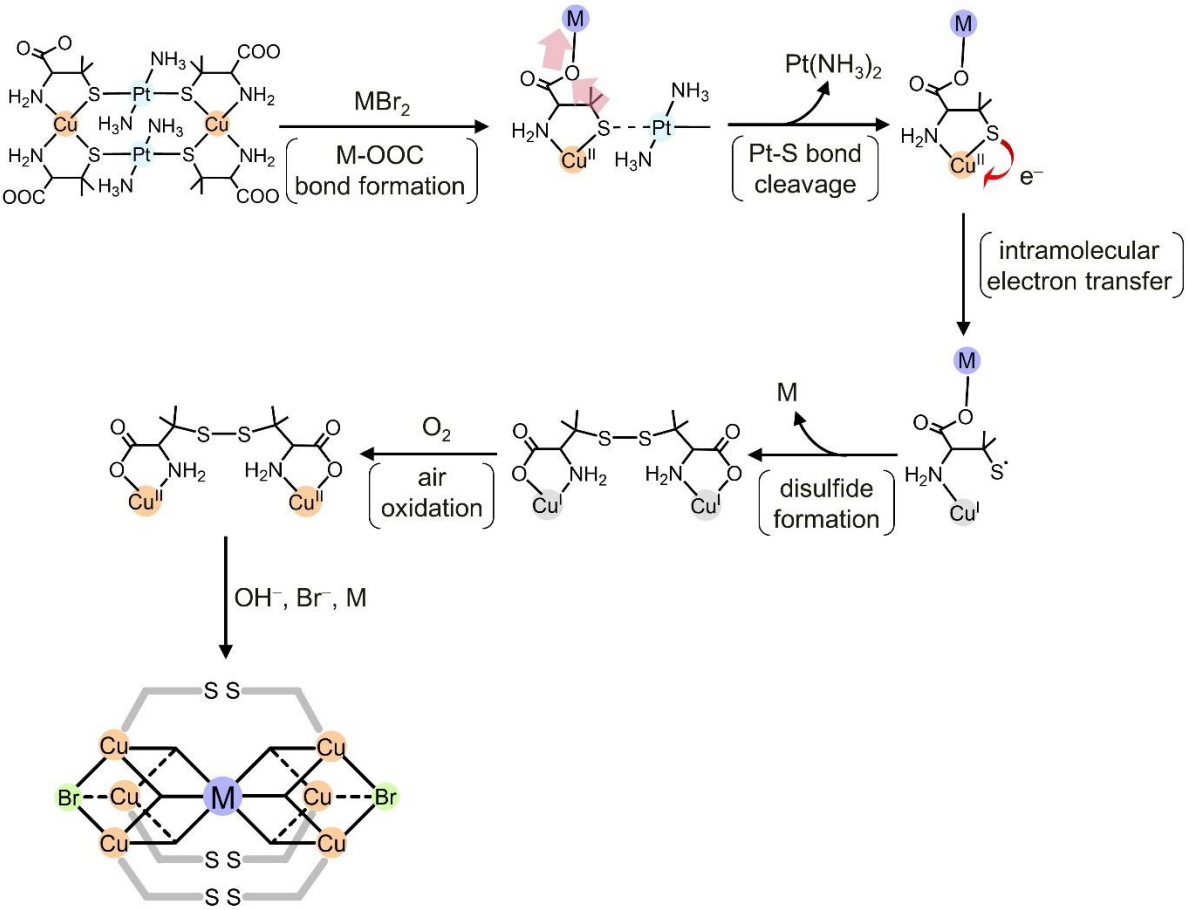

Fig. S7. Proposed mechanism of the formation of $\mathbf{1^{M}}$ (M = Mn^{II}, Co^{II}) from $[Cu_2Pt_2(NH_3)_4(D\text{-pen})_4]$ and MBr_2.

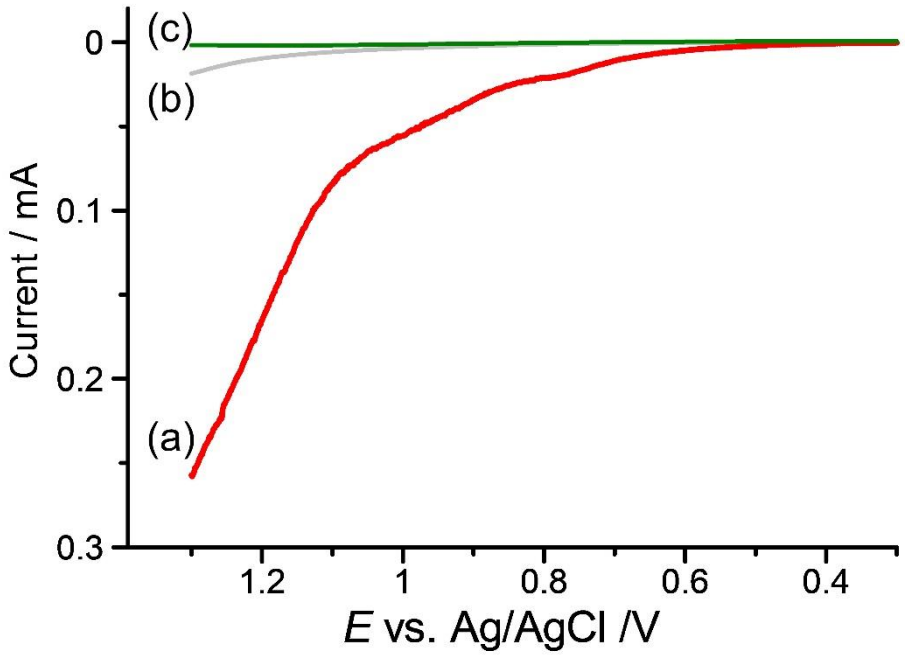

Fig. S8. Linear sweep voltammograms of (a) $\mathbf{1}^{Co}$, (b) a bare glassy carbon electrode in water containing 0.1 M LiOH as an electrolyte and (c) $\mathbf{1}^{Co}$ in acetonitrile containing 0.1 M LiOH as an electrolyte. The scan rate is 10 mV s^{-1}.

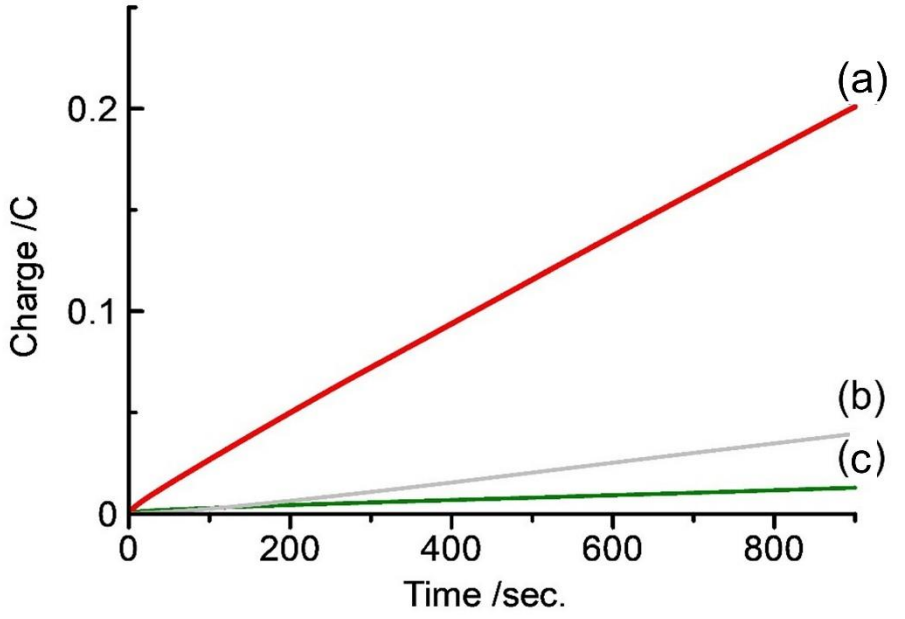

Fig. S9. Charge build-up vs. time in extended potential-controlled electrolysis of (a) $\mathbf{1}^{Co}$, (b) a bare glassy carbon electrode in aqueous 0.1 M LiOH solution and (c) $\mathbf{1}^{Co}$ in acetonitrile 0.1 M LiOH solution at an applied potential of +1.3 V.

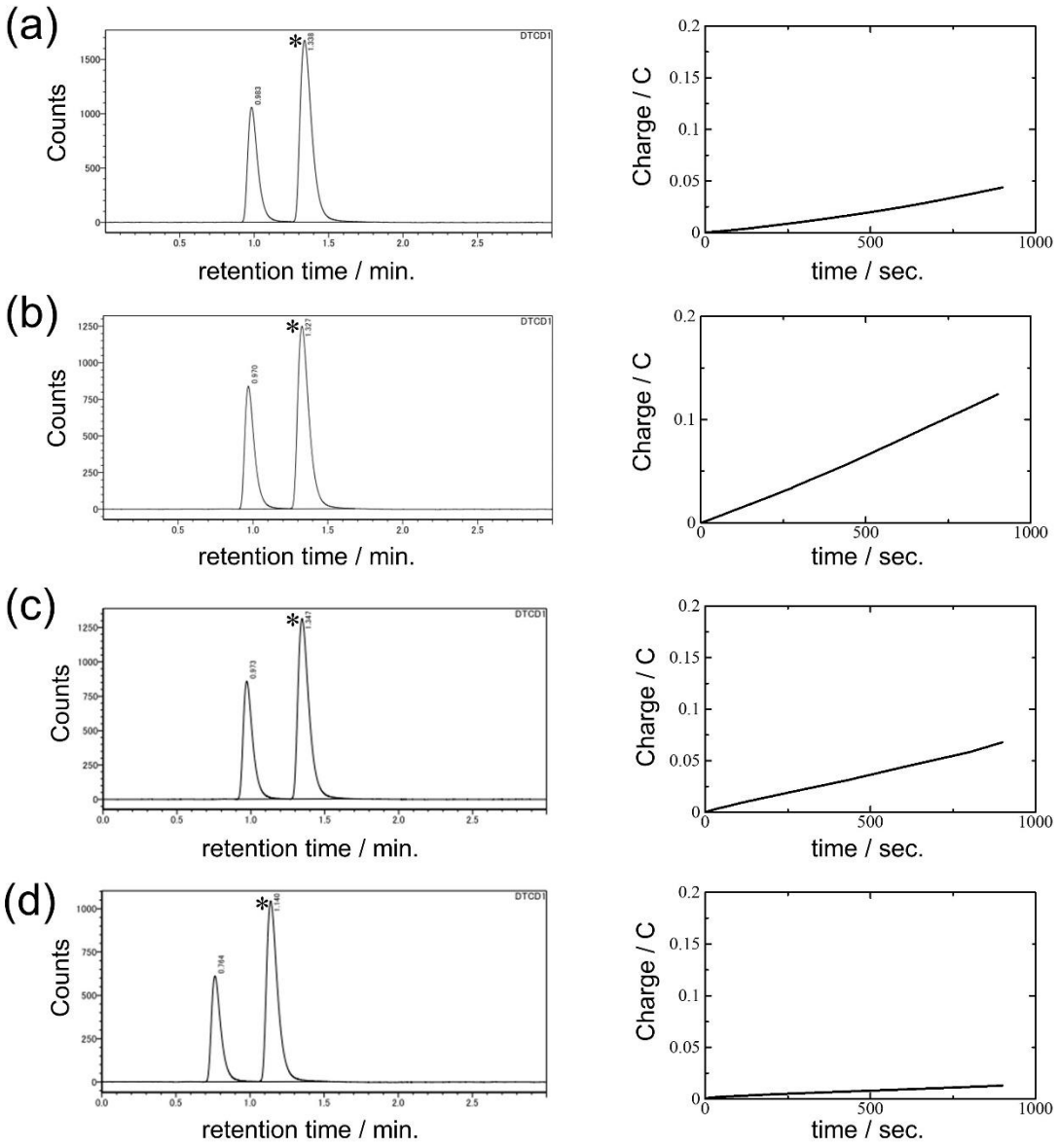

Fig. S10. (Left) Gas chromatogram of the head space after the electrolysis of (a) $\mathbf{1}^{\mathbf{Mn}}$, (b) $\mathbf{1}^{\mathbf{Co}}$, (c) $\mathbf{1}^{\mathbf{Cu}}$ and (d) blank attached to the glassy carbon electrode in 0.1 M LiOH aqueous solution at an applied voltage of +1.3 V for 15 min. (*) indicates N_2 gas contamination. (Right) Charge build-up vs. time plot of the electrolysis of (a) $\mathbf{1}^{\mathbf{Mn}}$, (b) $\mathbf{1}^{\mathbf{Co}}$, (c) $\mathbf{1}^{\mathbf{Cu}}$ and (d) blank.

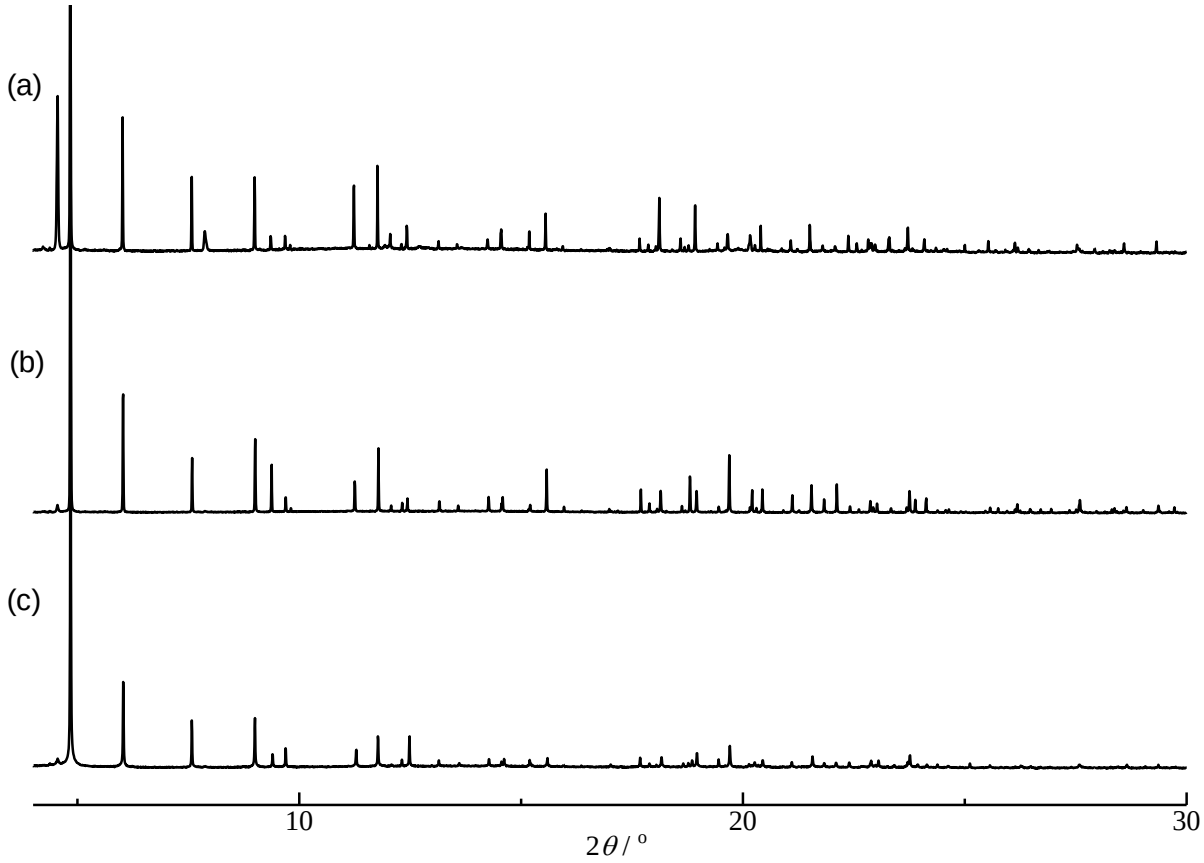

Fig. S11. PXRD patterns of (a) $\mathbf{1}^{\mathbf{Mn}}$, (b) $\mathbf{1}^{\mathbf{Co}}$ and (c) $\mathbf{1}^{\mathbf{Cu}}$ after bulk electrolysis at +1.3 V.

Table S1. Crystallographic data for $\mathbf{1^{Mn}}$ and $\mathbf{1^{Co}}$.

	$\mathbf{1^{Mn}}$	$\mathbf{1^{Co}}$
Formula	$C_{30}H_{101}Br_2Cu_6MnN_6O_{38.5}S_6$	$C_{60}H_{202}Br_4Cu_{12}Co_2N_{12}O_{77}S_{12}$
Colour, shape	blue, block	blue, block
M	1950.52	3909.02
Crystal system	Trigonal	Trigonal
Space group	$P3_2$	$P3_1$
a /Å	15.134(2)	15.0980(7)
b /Å	15.134(2)	15.0980(7)
c /Å	27.686(2)	55.4613(14)
α /°	90	90
β /°	90	90
γ /°	120	120
V /Å^3	5491.3(17)	10948.6(11)
Z	3	3
T /K	100	100
F(000)	2988	5988
ρ_{calcd} /g cm^{-3n}	1.769	1.779
μ /mm^{-1}	0.744	0.759
Crystal size /mm^3	0.14×0.08×0.08	0.08×0.06×0.05
Limiting indices	$-19 \le h \le 19$	$-19 \le h \le 19$
	$-19 \le k \le 19$,	$-18 \le k \le 19$,
	$-35 \le l \le 35$	$-72 \le l \le 72$
R_1[a] ($I>2\sigma(I)$)	0.0496	0.0399
wR_2[b] (all data)	0.1199	0.0892
GOF	1.148	0.892
Flack parameter	0.069(8)	0.046(10)
CCDC no.	2130570	2130571

[a] $R_1 = (\Sigma||F_o|-|F_c||)/(\Sigma|F_o|)$ [b] $wR_2 = [\{\Sigma w(F_o^2-F_c^2)^2\}/(\Sigma w|F_o^2|^2]^{1/2}$

Table S2. Average bond distances and angles of $\mathbf{1}^{Mn}$, $\mathbf{1}^{Co}$ and $\mathbf{1}^{Cu}$.

	$\mathbf{1}^{Mn}$	$\mathbf{1}^{Co}$ b)	$\mathbf{1}^{Cu}$
Bond distances (Å)			
M–O_{OH}	2.181(10)	2.117(14), 2.111(9)	2.2(3) (1.952(4), 1.956(4), 1.966(5), 1.986(4), 2.341(5), 2.781(5)) c)
Cu–O_{OH}	1.98(2)	1.976(16), 1.974(11)	1.98(3)
Cu–O_{COO}	1.96(2)	1.954(19), 1.950(14)	1.947(13)
Cu–N	1.994(5)	1.992(8), 1.991(6)	1.973(7)
Cu–Br	2.83(3)	2.84(5), 2.83(4)	2.82(8)
Angles (°)			
O–M–O (α) a)	75.6(8)	77.0(10), 76.7(5)	76(6) (68.67(16), 67.05(15), 82.95(18), 76.21(17), 75.94(17), 83.48(18)) c)
O–M–O (β) a)	90.0(13)	88.2(8), 88.7(10)	86(12) (69.81(13), 94.07(18), 95.53(18)) c)
O–M–O (γ) a)	139(4)	138(4), 138(5)	136(20) (114.74(16), 122.26(18), 123.58(16), 127.25(16), 161.11(19), 167.93(18)) c)
O_{OH}–Cu–O_{OH}	85.1(9)	83.7(6), 83.2(7)	84(2)
O_{OH}–Cu–O_{COO} (cis)	91.8(10)	92(2), 92.7(8)	91.2(10)
O_{OH}–Cu–O_{COO} (trans)	164(3)	165(2), 164(3)	164(5)
O_{OH}–Cu–Br	87.2(12)	87.0(13), 87.6(16)	87(2)
O_{COO}–Cu–Br	108(3)	108.0(16), 108(4)	108(4)
O_{OH}–Cu–N (cis)	99.0(16)	100(2), 100(2)	100(2)
O_{OH}–Cu–N (trans)	173.8(15)	174(2), 174.6(10)	172(3)
O_{COO}–Cu–N	83.2(5)	83.1(10), 83.1(7)	82.8(6)
Br–Cu–N	97(3)	95(3), 96(3)	96(4)

a) The O–M–O angles were defined as shown in the following figure:

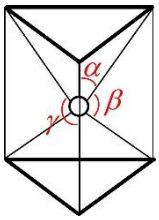

b) Crystal $\mathbf{1}^{Co}$ contains two independent complex molecules in one asymmetric unit.

c) The parenthetic numbers indicate the individual bond lengths and angles.

Table S3. Summary of the heterogeneous electrocatalytic activities for water oxidation.

Compound	Overpotential [a)]	TOF	FE	Ref. #
$\mathbf{1^{Mn}}$	537 mV	7.9 h^{-1}	50%	This work
$\mathbf{1^{Co}}$	237 mV	30 h^{-1}	85%	This work
$\mathbf{1^{Cu}}$	437 mV	23 h^{-1}	65%	This work
$[\{ZnCl(H_2O)\}(Cu_2\{Pt(NH_3)_2(D\text{-}pen)_2\}_2)]Cl$	133 mV	18 h^{-1} [b)]	15% [b)]	S1
$[Zn(Cu_2\{Pt(NH_3)_2(D\text{-}pen)_2\}_2)](ClO_4)_2$	133 mV	27 h^{-1} [b)]	86% [b)]	S1

a) The overpotentials were estimated based on the onset potential.

b) The bulk electrolysis experiments for TOF and FE calculations were carried out at an applied potential of +1.20 V (vs Ag/AgCl) in H_2O-CH_3CN (1:4) solution containing 0.1 M KPF_6 electrolyte.